Optical imaging of alpha emitters: simulations, phantom, and *in vivo* results

Federico Boschi
Sergio Lo Meo
Pier Luca Rossi
Riccardo Calandrino
Andrea Sbarbati
Antonello E. Spinelli

Optical imaging of alpha emitters: simulations, phantom, and *in vivo* results

Federico Boschi,[a] **Sergio Lo Meo,**[b] **Pier Luca Rossi,**[c] **Riccardo Calandrino,**[d] **Andrea Sbarbati,**[a] **and Antonello E. Spinelli**[d]

[a]University of Verona Department of Neurological, Neuropsychological, Morphological and Motor Sciences, Strada Le Grazie 8, 37134 Verona, Italy
[b]Ionizing Radiation Laboratory, National Institution for Insurance against Accidents at Work (INAIL), Via Fontana Candida 1, I-00040, Monte Porzio Catone, Rome, Italy
[c]University of Bologna, Department of Physics, Viale Berti Pichat 6/2, Bologna, Italy
[d]San Raffaele Scientific Institute, Medical Physics Department, Via Olgettina N. 60, Milan, Italy

Abstract. There has been growing interest in investigating both the *in vitro* and *in vivo* detection of optical photons from a plethora of beta emitters using optical techniques. In this paper we have investigated an alpha particle induced fluorescence signal by using a commercial CCD-based small animal optical imaging system. The light emission of a ^{241}Am source was simulated using GEANT4 and tested in different experimental conditions including the imaging of *in vivo* tissue. We believe that the results presented in this work can be useful to describe a possible mechanism for the *in vivo* detection of alpha emitters used for therapeutic purposes. © *2011 Society of Photo-Optical Instrumentation Engineers (SPIE)*. [DOI: 10.1117/1.3663441]

Keywords: fluorescence; biology; medicine; biomedical optics.

1 Introduction

Recently, there has been a growing interest in investigating both the *in vitro* and *in vivo* detection of optical photons from a plethora of radioisotopes using CCD detectors. In earlier works, particular attention has been focused on the detection of Cerenkov photons from beta plus emitters;[1–5] these studies have shown that the spectrum of the emitted optical photons follows the predicted $1/\lambda^2$ shape, typical of the Cerenkov radiation (CR). It is well-known that the emission of CR takes place only when charged particles travel in the medium with a velocity greater than the speed of light in the medium. The energy threshold for CR emission is thus dependent on the medium and, for example, the threshold for a beta particle traveling in water is 263 keV. In the last year, the investigation of weak optical emission coming from a pure gamma emitter such as Tc-99 m was also reported.[6]

One recent study has shown the detection of an intense light emission when using an alpha emitter such as ^{225}Ac.[5] In this case given the mass of the alpha particles, the generation of optical photons cannot be explained in terms of Cerenkov effect and, thus, alternative explanations are needed. For example, in Ref. 5 it has been suggested that even if the origin of optical emission from ^{225}Ac is uncertain it can be linked to CR emitted from the beta minus short-lived daughter nuclides such as ^{213}Bi. This appears to be a plausible and interesting hypothesis; however, a more general explanation of the intense light emission of ^{225}Ac can be the combination of both Cerenkov photons generated by the beta particles emitted by daughter nuclides and fluorescence induced by alpha particles. The main goal of this proof of principle work was to investigate the latter effect in different experimental conditions.

The detection of ultraviolet fluorescence light emission from nitrogen due to interactions with alpha particles in the atmosphere was investigated, for example, in Ref. 7 and applied to nuclear safeguard issues.

In this paper we have investigated alpha particle induced fluorescence signal by using GEANT4 Monte Carlo (MC) simulations and a commercial CCD-based small animal optical imaging system. More precisely, we measured the light emission induced by a ^{241}Am source in different experimental conditions including the imaging of *in vivo* tissue. This isotope is interesting since the principal decay modes of ^{241}Am are mainly alpha emission and low energy gamma radiations. The decay product of ^{241}Am is ^{237}Np which has a long half-life equal to 2.1×10^6 years. These physical properties of ^{241}Am are quite useful since they allow us to exclude any possible contribution from Cerenkov light photons generated by high energy electrons and, thus, gave us the possibility to estimate the contribution of alpha particles induced fluorescence only. We believe that the results presented in this work can be useful to describe a possible alternative mechanism for the *in vivo* detection of alpha emitters used for therapeutic purposes.

For the sake of clarity, in order to distinguish between Cerenkov luminescence imaging and luminescence induced by non-Cerenkov mechanisms we use here the more general term of radioluminescence imaging (RLI).

2 Materials and Methods

2.1 RLI Simulation and Acquisition in Air and Under a Plexiglas Slab

RLI images of 5-mm diameter ^{241}Am source (The Radiochemical Centre, Amersham) with an activity equal to 70 kBq placed in

Address all correspondence to: Federico Boschi, University of Verona, Department of Neurological, Neuropsychological, Morphological and Motor Sciences, Strada Le Grazie 8, 37134 Verona, Italy. Tel: 0458027272; E-mail: federico.boschi@univr.it.

air were acquired by using the IVIS 200 optical imager (Caliper Life Sciences, Alameda, USA). The IVIS 200 is based on a cooled ($-90°C$) back-thinned, back-illuminated CCD camera. The CCD has an active array of 1920×1920 pixels with a dimension of 13 μm.

RLI spectral data of the ^{241}Am source in air were measured by acquiring six images with the narrow band (FWHM $\sim$20 nm) emission filters (centered on 560, 580, 600, 620, 640, and 660 nm) with the following parameters: exposure time $= 300$ s, $f = 1$, binning $B = 8$ or 32, and with a field of view $= 12.8$ cm. Images were acquired and analyzed with Living Image 4.0 (Caliper Life Sciences) and were corrected for dark measurements.

A lateral image of the fluorescence of air induced by alpha particles were also investigated by placing the source close to a 45 deg mirror and the corresponding image was then focused on the CCD detector. In order to further understand the origin of fluorescence, a small piece of carton (1-mm thick, black carton, Strathmore) was placed 1 cm above the ^{241}Am source, to stop a fraction of the emitted alpha particles. A lateral image of this experimental setup was acquired to show the missing optical signal in the region above the carton.

Similar to the acquisition of RLI images in air, the ^{241}Am source was placed under a 2.5 slab of Plexiglas. The average radiance (p/s/cm^2/sr) at different wavelengths was then obtained by placing a small region of interest (ROI) over the source.

The Monte Carlo GEANT4[8] (4.9.0 version) was used for simulation air fluorescence. The simulated setup consisted of a cylinder (10 μm height; 2.5 mm radius) homogeneously filled with ^{241}Am placed on a aluminium cylinder (1 mm height; 7.5 mm radius). A thin detector, with a efficiency of 85% for optical photons in the range from 1.4 to 3.1 eV, is placed perpendicular to the base of the ^{241}Am source and in contact with it. The simulation of the electromagnetic interactions was made by using the "EM Standard" library, while for nuclear decays GEANT4 provided a G4RadioactiveDecay class to simulate the full disintegration of radioactive nuclei by α, $\beta+$, $\beta-$ emissions and electron capture. The simulation model is empirical and data-driven, and uses the Evaluated Nuclear Structure Data File[9] to obtain all the information about: nuclear half-lives, nuclear level structure for nuclides, decay branching ratios, and energy of the decay process. In the event that a nuclide obtained by a nuclear decay is an excited isomer, its prompt nuclear de-excitation is treated by using the G4PhotoEvaporation class. The air fluorescence was simulated by a light yield factor equal to seven optical photons for each MeV (Ref. 8) of energy deposited by alpha particles crossing the air.

2.2 RLI Acquisition In Vivo

In order to investigate the luminescence *in vivo*, the ^{241}Am source was placed under a mouse shoulder; the animal was a control nude mouse of 25 g. The amount of tissue above the source was 2 to 3 mm. Even if this cannot be considered as a true physiological condition, it allowed us to investigate under known setting, e.g., source position, radioisotope activity, and tissue thickness, the signal due to tracer accumulation in a superficial region of the animal. RLI spectral data *in vivo* were measured by acquiring six images with the narrow band emission filters as described in Sec. 2.1. During image acquisition the mouse was kept under gaseous anesthesia (2% of isoflurane and 1 l/min of oxygen). All the animal handling was approved by the Institutional Ethical Committee according to the regulations of the Italian Ministry of Health and to the European Communities Council (86/609/EEC) directives. Analogously to Sec. 2.1, the average radiance at the different wavelengths was obtained by tracing on the images a small ROI around the source.

3 Results

3.1 RLI Simulation and Acquisition in Air and Under a Plexiglas Slab

Figure 1(a) shows a frontal RLI of the ^{241}Am source placed in air. Figure 1(b) shows the radiance profiles in the horizontal (x) and vertical (y) directions at the center of the source.
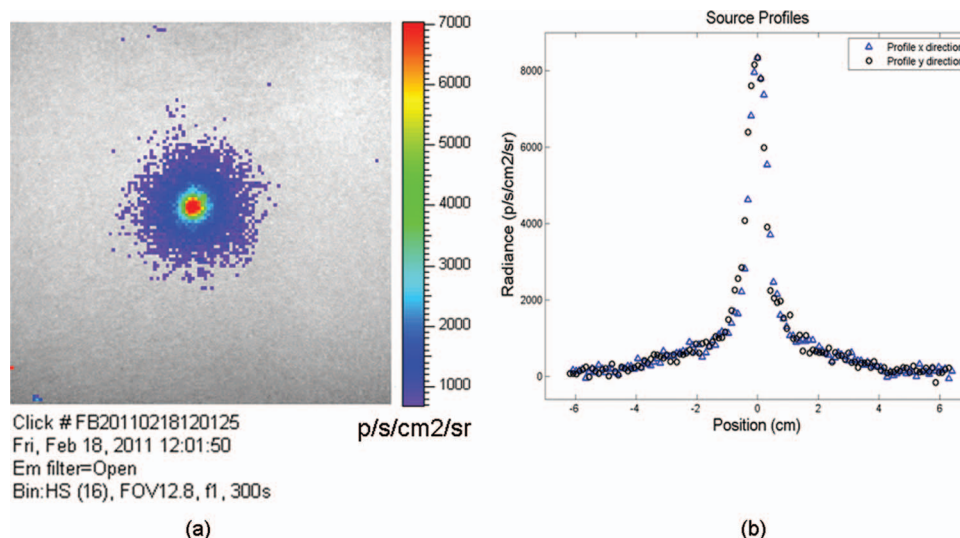

Click # FB20110218120125
Fri, Feb 18, 2011 12:01:50
Em filter=Open
Bin:HS (16), FOV12.8, f1, 300s

(a)

(b)

Fig. 1 (a) RLI image of the ^{241}Am source in air. (b) The corresponding radiance (p/s/cm^2/sr) profiles in the *x-y* directions at the center of the source.
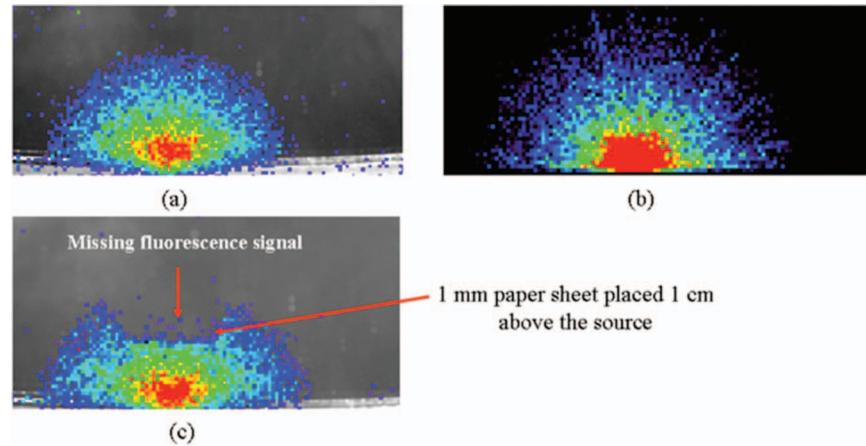
Fig. 2 Lateral view (obtained using a mirror) of the ^{241}Am source in air. (a) and (b) show, respectively, experimental and MC simulated data. (c) The resulting fluoresce image obtained by using a 1 mm sheet of carton positioned 1 cm above the source. The arrows point at the area above the sheet of carton where there is a clear loss of light signal.

By looking at the profiles in Fig. 1(b) one can deduce that the total luminescence signal is a sum of localized intense emission in the active part of the source and a much broader signal. The broader component of the luminescence signal is about 4-cm long, matching quite well the ^{241}Am alpha particles range in air.

A lateral view of the air fluorescence induced by the ^{241}Am source is presented in Fig. 2. Figure 2(a) shows the light signal generated by alpha particles. The corresponding Monte Carlo simulations shown in Fig. 2(b) fits qualitatively well with the experimental findings. Figure 2(c) shows the fluorescence image obtained by stopping a fraction of alpha particles with a piece of carton as described in Sec. 2. As one can notice by comparing Fig. 2(a) with Fig. 2(c), there is a clear reduction of the fluorescence light signal above the region covered by the carton. This is a rather simple but useful way to show that the causes of the air fluorescence were mainly alpha particles emitted by the ^{241}Am source.

Figure 3(a) shows the luminescence after covering the alpha source with a Plexiglas slab. In this case the spread of the alpha particles emitted by the ^{241}Am source is negligible and the light is localized only above the active part of the source.

The images obtained by covering the alpha source with a piece of carton in Fig. 3(b) show a negligible signal in the Plexiglas; this is clear evidence that the main cause of the light was the fluorescence of the source.

The spectra of the light obtained when placing the source in air and under a 2.5 mm Plexiglas slab are shown in Fig. 4.

The spectra in Fig. 4 present different shapes and intensities depending on the materials. It is important to underline here that because the spectra contains only 6 points this cannot be considered to be a detailed precise spectral measurements, and, thus, Fig. 4 provides a rough estimate of the emission spectra of both air and Plexiglas.

3.2 *In Vivo RLI*

An *in vivo* image of luminescence induced by an alpha particle source in a mouse is shown in Fig. 5(a). It is interesting to notice that the fluorescence signal can be clearly seen inside the red ROI even if the source activity is quite modest.

Another interesting aspect is that the source signal is well localized under the mouse shoulder, suggesting a reasonably precise spatial delineation of the luminescence emission region.
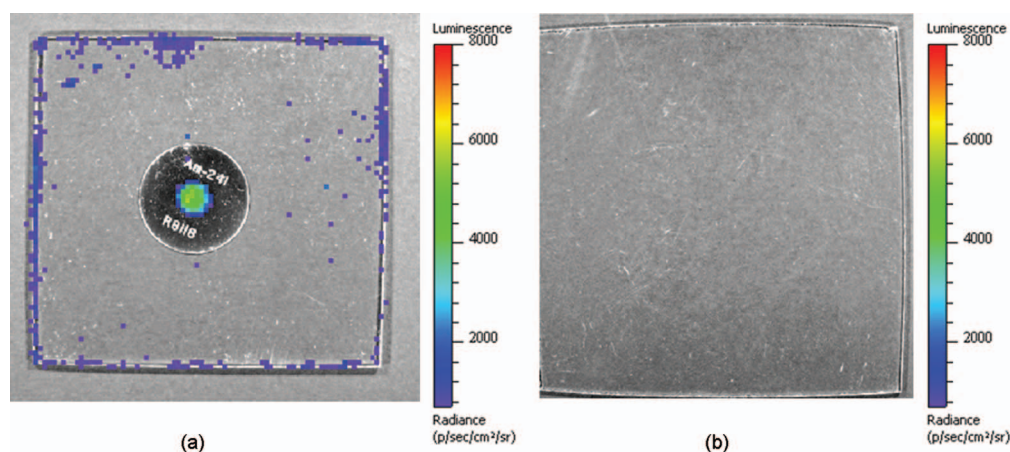

Fig. 3 (a) An RLI image of the ^{241}Am source under 2.5 mm of Plexiglas. (b) The source was covered with a 1-mm thick piece of carton.
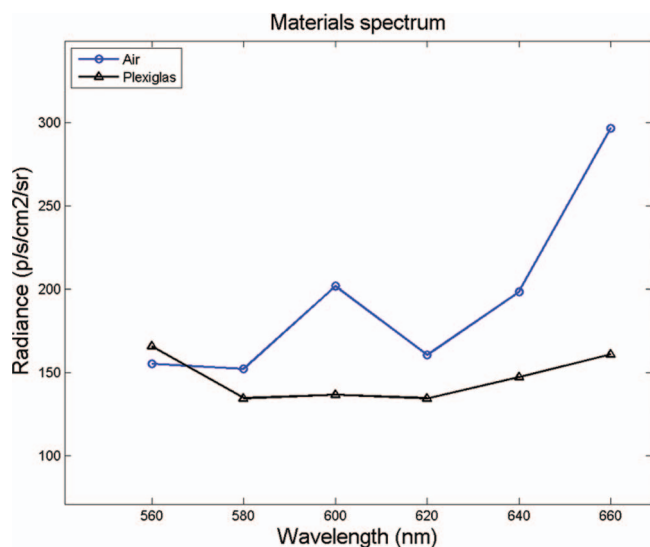
Fig. 4 RLI spectrum of the ^{241}Am source in air (circles) and Plexiglas (square). The spectra were acquired as described in Sec. 2.1.

4 Discussions and Conclusions

The results presented in Sec. 3 showed that the light emission of an alpha particles source can be detected using a commercial small animal optical imaging system. Such systems are becoming widely available in biology and preclinical imaging laboratories and, thus, we believe that the results presented in this work will help to expand their range of applications.

The broad component of the radiance profiles shown in Fig. 1(b) clearly underlines a direct link between the known alpha particles range in air and the extension of the region where the fluoresce light is emitted. The experiment performed by stopping a fraction of the alpha particles (see Fig. 2) confirms as well that the origin of the fluorescence signal are the alpha particles emitted by the ^{241}Am source.

The output of Monte Carlo simulations qualitatively agreed with the experimental data obtained by imaging the alpha source in the air. This is quite an interesting aspect of the work that needs to be further developed to simulate, for example, more complex conditions. In this paper the main goal of the MC simulations was to further investigate the cause of the detected fluorescence signal in air. A quantitative comparison between the measured and simulated data was not our priority and was not possible since we did not have a detailed scheme of the imaging apparatus to be implemented in the MC simulations.

Plexiglas and *in vivo* tissue showed a different light output response both in terms of magnitude and spectral output. As already mentioned in Sec. 3 the measured spectra using the IVIS 200 can be considered as an evaluation of the true emission spectra. A detailed spectral analysis requires the use of a dedicated spectrometer and is well beyond the scope of this paper since our main goal here was to investigate the use of a CCD-based commercial small animal optical imaging system.

In vivo investigation of alpha particles tissue interactions is shown in Sec. 3.2, in particular Fig. 5 provides a clear evidence that alpha source induces a well localized luminescence signal in a mouse tissues. Obviously the generated light photons will suffer from scattering analogously to conventional luminescence imaging, and, thus, the *in vivo* spatial resolution will ultimately be dependent on this effect.

In our opinion the most interesting aspect of the work presented here is the proof of concept that alpha emitters with no beta emission can be imaged *in vivo* using standard optical imaging methods commonly used for preclinical experiments.

Most of the alpha emitters used for therapeutic applications also emit gamma rays and, thus, they can be imaged using SPECT; however the percentage of gamma emission is rather low, typically being a few percent of the total decays. This might increase significantly the acquisition time and requires expensive dedicated hardware with respect to optical imaging.

As shown by Miederer et al.[10] the preclinical study of biodistribution of 225Ac-DOTATOC for neuroendocrine tumor model was performed by scarifying the animals and then counting
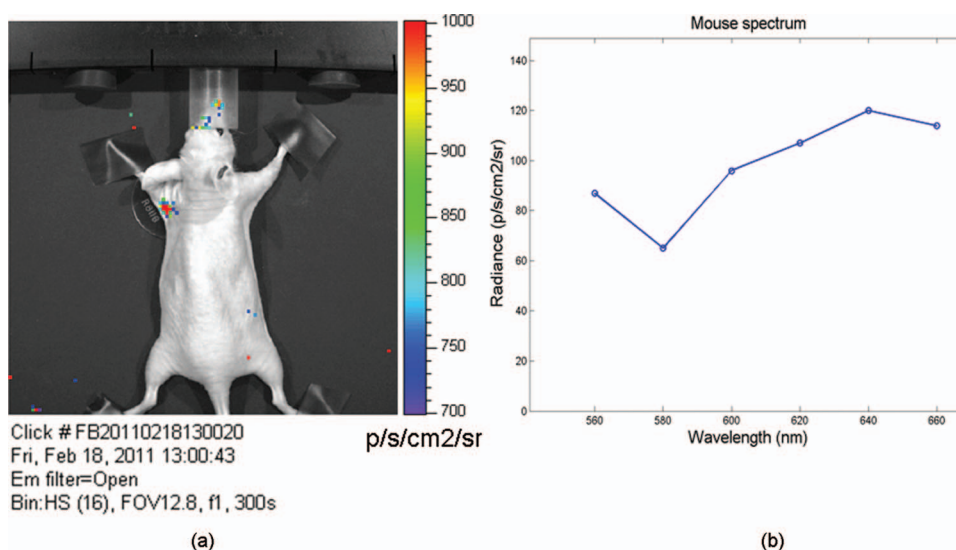

Fig. 5 (a) RLI image of the ^{241}Am source (white arrow) placed under a control nude mouse (25 g). The spectrum of the emitted light by the animal at the center of the red ROI can be found in (b).

the organs with a gamma counter. Our optical imaging method could be used to image at different time points the same animal, and, thus without scarifying them. This will allow the reduction of the number of animals used for preclinical protocols and more importantly to provide a better understanding, in a truly molecular imaging sense, of the *in vivo* alpha emitters biodistribution.

This is quite an important and useful aspect because by using the RLI approach we hypothesize it will be possible to perform cost effective preclinical studies of new radiopharmaceuticals, and to infer more precisely the therapeutic outcomes by imaging directly the biodistribution of molecules labeled with alpha emitters.

Future work will be focused on this direction more precisely to develop xenograft mouse tumor models and to use the RLI approach to image the tumor progression.

Acknowledgments

References

1. R. Robertson, M. S. Germanos, C. Li, G. S. Mitchell, S. R. Cherry, and M. D. Silva, "Optical imaging of Cerenkov light generation from positron-emitting radiotracers," *Phys. Med. Biol.* **54**, N355–N365 (2009).
2. A. E. Spinelli, D. D'Ambrosio, L. Calderan, M. Marengo, A. Sbarbati, and F. Boschi, "Cerenkov radiation allows *in vivo* optical imaging of positron emitting radiotracers," *Phys. Med. Biol.* **55**, 483–495 (2010).
3. F. Boschi, L. Calderan, D. D'Ambrosio, M. Marengo, A. Fenzi, R. Calandrino, A. Sbarbati, and A. E. Spinelli, "*In vivo* (18)F-FDG tumour uptake measurements in small animals using Cerenkov radiation," *Eur. J. Nucl. Med.* **38**, 120–127 (2011).
4. A. E. Spinelli, F. Boschi, D. D'Ambrosio, L. Calderan, M. Marengo, A. Fenzi, A. Sbarbati, A. Del Vecchio, and R. Calandrino, "Cerenkov radiation imaging of beta emitters: *In vitro* and *in vivo* results," *Nucl. Instr. Meth. A* **648**, S310–S312 (2011).
5. A. Ruggiero, J. P. Holland, J. S. Lewis, and J. Grimm, "Cerenkov luminescence imaging of medical isotopes," *J. Nucl. Med.* **51**, 1123–1130 (2010).
6. A. E. Spinelli, S. Lo Meo, R. Calandrino, A. Sbarbati, and F. Boschi, "Optical Imaging of Tc-99m based tracers, *in vitro* and *in vivo* results," *J. Biomed. Opt.* (in press).
7. S. M. Baschenko, "Remote optical detection of alpha particle sources," *J. Rad. Prot.* **24**, 75–82 (2004).
8. S. Agostinelli, J. Allison, K. Amako, J. Apostolakis, H. Araujo, P. Arce, M. Asai, D. Axen, S. Banerjee, G. Barrand, F. Behner, L. Bellagamba, J. Boudreau, L. Broglia, A. Brunengo, H. Burkhardt, S. Chauvie, J. Chuma, R. Chytracek, G. Cooperman, G. Cosmo, P. Degtyarenko, A. Dell'Acqua, G. Depaola, D. Dietrich, R. Enami, A. Feliciello, C. Ferguson, H. Fesefeldt, G. Folger, F. Foppiano, A. Forti, S. Garelli, S. Giani, R. Giannitrapani, D. Gibin, J. J. Gómez Cadenas, I. González, G. Gracia Abril, G. Greeniaus, W. Greiner, V. Grichine, A. Grossheim, S. Guatelli, P. Gumplinger, R. Hamatsu, K. Hashimoto, H. Hasui, A. Heikkinen, A. Howard, V. Ivanchenko, A. Johnson, F. W. Jones, J. Kallenbach, N. Kanaya, M. Kawabata, Y. Kawabata, M. Kawaguti, S. Kelner, P. Kent, A. Kimura, T. Kodama, R. Kokoulin, M. Kossov, H. Kurashige, E. Lamanna, T. Lampén, V. Lara, V. Lefebure, F. Lei, M. Liendl, W. Lockman, F. Longo, S. Magni, M. Maire, E. Medernach, K. Minamimoto, P. Mora de Freitas, Y. Morita, K. Murakami, M. Nagamatu, R. Nartallo, P. Nieminen, T. Nishimura, K. Ohtsubo, M. Okamura, S. O'Neale, Y. Oohata, K. Paech, J. Perl, A. Pfeiffer, M. G. Pia, F. Ranjard, A. Rybin, S. Sadilov, E. Di Salvo, G. Santin, T. Sasaki, N. Savvas, Y. Sawada, S. Scherer, S. Sei, V. Sirotenko, D. Smith, N. Starkov, H. Stoecker, J. Sulkimo, M. Takahata, S. Tanaka, E. Tcherniaev, E. Safai Tehrani, M. Tropeano, P. Truscott, H. Uno, L. Urban, P. Urban, M. Verderi, A. Walkden, W. Wander, H. Weber, and J. P. Wellisch, "Geant4: a simulation toolkit," *Nucl. Instrum. Meth. A* **506**, 250–303 (2003).
9. J. Tuli, "Evaluated Nuclear Structure Data File," BNL-NCS-51655-Rev87 (1987).
10. M. Miederer, G. Henriksen, A. Alke, I. Mossbrugger, L. Quintanilla-Martinez, R. Senekowitsch-Schmidtke, and M. Essler, "Preclinical evaluation of the α-particle generator nuclide 225Ac for somatostatin receptor radiotherapy of neuroendocrine tumors" *Clin. Cancer Res.* **14**, 3555–3561 (2008).